Semi-Annual Report of Activities for

NASA NGR 33-008-037

# Program of Research in Theoretical and Experimental Geology and Geophysics in Areas of Direct Interest to the NASA Space Science Program

P. W. Gast
Principal Investigator

January 26, 1967

During the period beginning July 1, 1966, funds supplied by this grant have been primarily used to support the activities of a number of graduate students. Reports of their individual research projects are given in short Appendices to this report. In addition, the work of Dr. W. M. Compston, a Resident Research Associate in the Institute for Space Studies was supported. Results of his ten month study are included in Appendix A. Dr. Menachim Dishon, a Resident Research Associate at the Institute for Space Studies during 1964 and 1965 was also supported. A brief summary of his work is given in Appendix G.

# ISOTOPE COMPOSITION OF LEAD IN TEKTITES

W. M. Compston and P. W. Gast

The lead and uranium content and lead isotope composition has been determined in a group of ten tektites from Australia, Indo-China and the Philippines. Results of this study are summarized in Tables 1 and 2 and in Figure 1. All isotope compositions are normalized to a constant $Pb^{206}/Pb^{208}$ value in an isotope standard prepared from enriched isotopes. The precision of these data is $\pm$ 0.2% or better for ratios $Pb^{206}/Pb^{208}$, $Pb^{206}/Pb^{207}$ and better than $\pm$ 0.3% for the $Pb^{206}/Pb^{204}$ ratio. Even though the occurrence of the tektite samples used covers a very wide area, they form a very homogeneous group with respect to their U content and Pb isotope composition. The Pb isotope composition does not preclude their being formed from recent soils or sediments. The high $U^{238}/Pb^{204}$ ratio strongly suggests that Pb was volatilized from the glass. It is not consistent with the observed Pb isotope composition or with the observed U values for terrestrial materials.

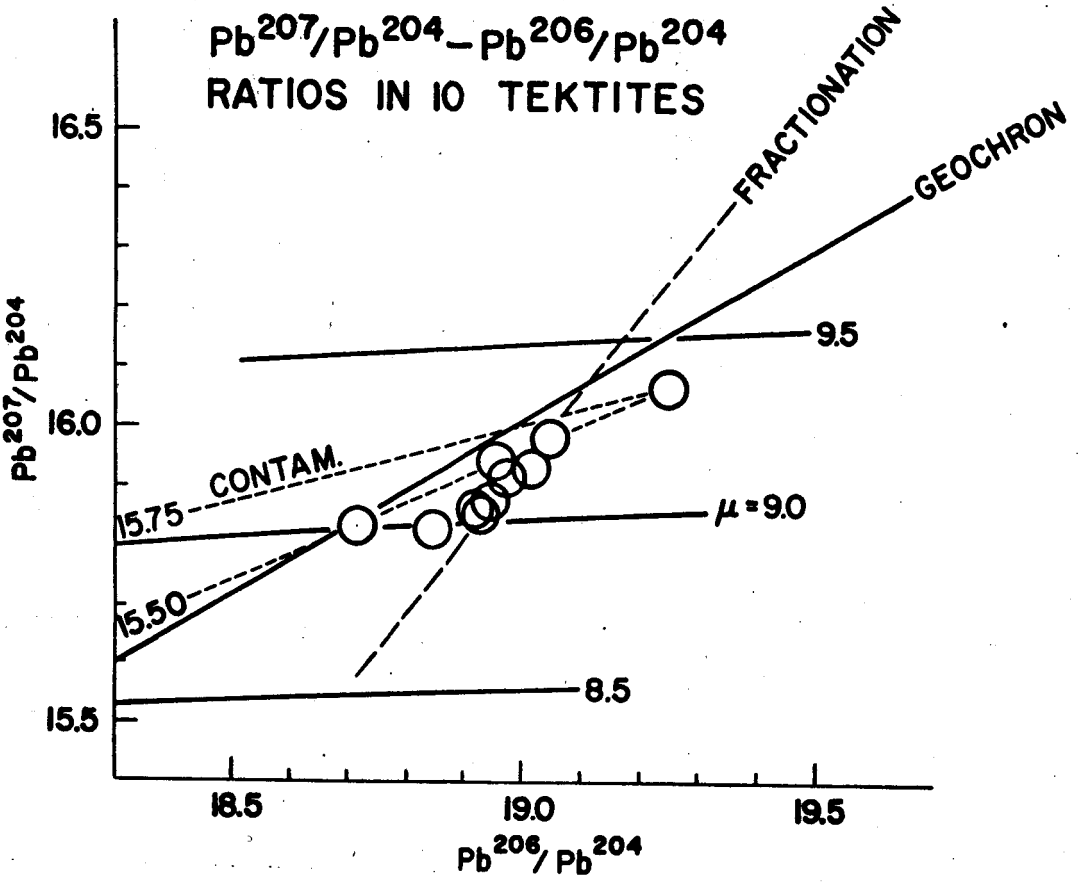
Pb207/Pb204–Pb206/Pb204
RATIOS IN 10 TEKTITES
FRACTIONATION
GEOCHRON
9.5
CONTAM.
15.75
μ=9.0
15.50
8.5
16.5
16.0
15.5
Pb207/Pb204
18.5
19.0
19.5
Pb206/Pb204

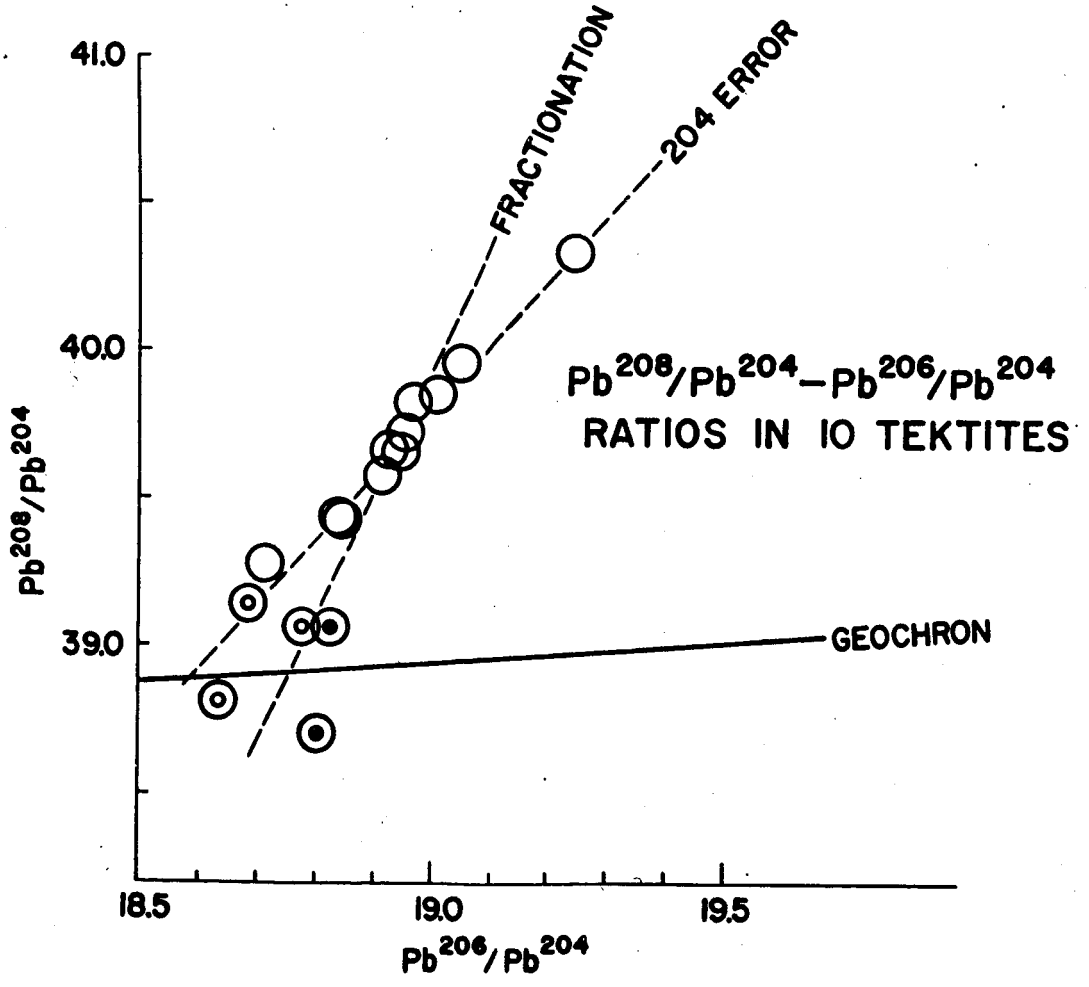
FRACTIONATION
204 ERROR
Pb208/Pb204–Pb206/Pb204
RATIOS IN 10 TEKTITES
GEOCHRON
41.0
40.0
39.0
Pb208/Pb204
18.5
19.0
19.5
Pb206/Pb204

## Lead and Uranium Content in Australasian Tektites

| Specimen | U (ppm) | Pb (ppm) | $U^{238}/Pb^{204}$ |
|---|---|---|---|
| Australites | | | |
| DA 43 ) | 2.45 | 4.33 | 36.9 |
| DA 415 ) | 2.45 | 5.63 | 29.0 |
| DA 45 ) | 1.99 | 2.77 | 47.2 |
| WMC | 1.97 | 4.55 | 28.7 |
| T 98 ) | 2.32 | 5.09 | 35.7 |
| EH ) | 2.55 | 4.23 | 39.1 |
| Philippinites | | | |
| T 66A ) | 2.62 | 4.46 | 38.2 |
| P 66 ) | 2.61 | 4.57 | 36.9 |
| EC 1 ) | 2.63 | 6.69 | 25.8 |
| EC 2 ) | 2.39 | 4.41 | 35.3 |
| CRT | 2.80 | 6.44 | 28.4 |

Isotope Composition of Lead in Australasian Tektites

| Specimen | 206/204 | 207/204 | 208/204 |
|---|---|---|---|
| Australites | | | |
| DA 43 ) | 18.946 | 15.878 | 39.67 |
| DA 415 ) | 18.934 | 15.851 | 39.67 |
| DA 45 ) | 19.054 | 15.985 | 39.96 |
| WMC | 19.250 | 16.065 | 40.34 |
| T 98 ) | 18.975 | 15.915 | 39.83 |
| EH ) | 18.849 | 15.830 | 39.43 |
| Philippinites | | | |
| T 66A ) | 18.848 | 15.827 | 39.43 |
| P 66 ) | 18.718 | 15.836 | 39.28 |
| EC 1 ) | 19.019 | 15.928 | 39.86 |
| EC 2 ) | 18.922 | 15.862 | 39.58 |
| CRT | 18.959 | 15.946 | 39.73 |

# REPORT OF SUMMER STUDENT ACTIVITIES

During the summer of 1966, three students selected from a group of approximately fifty applicants were employed in the Geochemistry Laboratory of the Lamont Geological Observatory. They were: 1) George Atkinson, Florida Presbyterian University, 2) Morris Drucker, Department of Chemistry, Columbia University and 3) Rudy Richardson, Wichita State University.

1) Atkinson continued work begun during the previous summer by another student developing a mass spectrometric technique for the determination of Zr in meteorites and rocks.

2) Drucker, an undergraduate student at Columbia University, investigated the disequilibrium in the uranium and thorium series in a core from Great Salt Lake. The goal was to obtain sedimentation rates using the ionium and potassium methods similar to those used in the ocean. He found that the system was largely detrital material, and he was unable to separate a useful authigenic portion.

3) Richardson, a student at Wichita State University, Kansas, attempted to measure the carbon and oxygen isotope fractionation factor between $CO_2$ gas and the surface molecular of some common carbonate minerals at 200-300°C. Oxygen isotopic fractionation among carbonates and between carbonates and water is temperature dependent and is often used as a geologic thermometer. It would be important to determine the possibility of isotopic fractionation between the surface molecules and interior of carbonates, since depending on the relative rates of crystal growth and oxygen diffusion, fluid phases equilibrating with carbonates may only effectively "see" the surface molecular layer.

Preprint of a paper by Lawrence Neuman to be submitted to the Journal of Geophysical Research.

# THERMAL HISTORY OF THE MOON FOR NON-CHONDRITIC URANIUM AND POTASSIUM CONTENTS

Lawrence Neuman
Lamont Geological Observatory of Columbia University
Palisades, New York

The thermal evolution of both the Earth and the Moon has been previously calculated by Urey (1952, 1962), MacDonald (1959), Jacobs (1956), Lubimova (1958) and others. The usual radioactive composition that was chosen in these studies is that of chondritic meteorites. MacDonald showed that this choice for the Earth enabled him to reproduce the observed heat flow at the surface of our planet.

Gast (1960), Wasserberg et al. (1964), Tilton and Reed (1963) and Urey (1964) argue against the use of a chondritic composition in the case of the Earth. MacDonald (1964) calculated non-chondritic models for the Earth in which the ratio of potassium to uranium was reduced from the chondritic value of $8 \times 10^4$ to $1 \times 10^4$. The decrease in radioactivity was balanced by raising the absolute amount of uranium from .01 ppm to .04 ppm. Here again, the terrestrial heat flow values could be reproduced.

Lunar studies by Urey (1959) using the chondritic composition and Phinney and Anderson (1965) using the so-called Wasserberg composition showed that the Moon in both cases would melt extensively,early in its history. The object of the present study was to determine the thermal history of the Moon based upon a model in which the chondritic radioactivity was allowed to include a range of uranium concentrations (U = .001, .01, .04 ppm) and K/U ratios ($5 \times 10^3$, $1 \times 10^4$, $2 \times 10^4$). With this range of values, limits can be set on the required initial concentrations of radioactive materials and temperature distributions within the Moon to produce melting over a period of $4.5 \times 10^9$ years.

A simple lunar model was chosen following that of Urey (1959). The model Moon chosen is spherically symmetrical with a homogenous distribution of radioactive materials. The lattice conductivity is constant in the calculation and the latent heat of melting is not considered. This neglect of radiative heat transport and latent heat requirements allow melting to take place at lower temperatures than are physically realizable. Hence, when melting is avoided in a specific model, the given radioactive content is a lower limit, and greater heat is actually required.

The initial temperature distribution plays a significant but not a dominant part in determining the subsequent development of the temperature profile. The temperature distribution was assumed to fall off as an inverse function of the radius squared:

$T = T_0 \left( 1 - \left(\frac{r}{R}\right)^2 \right)$ where R = lunar radius = 1738 km

and $T_0$ = the temperature at the center of the Moon

To include the possibilities that the Moon may have formed at either low temperatures or high temperatures, a range of initial $T_0$'s were chosen = 0°C, 600°C, 1000°C, 1500°C.

The solution of the differential equation for heat flow in a spherically symmetric body with uniform heating and constant coefficient of thermal conductor followed that of Carslaw and Jaeger. Numerical evaluation was performed on the IBM 7094.

Results of some of the calculations are presented in Figures 1 and 2. Figure 1 is a temperature versus depth plot with $T_0$ = 600°C and is a representation of the possible thermal structure in the present-day Moon. With the uranium content as parameter, temperature is plotted from the surface to the center after $t = 4.5 \times 10^9$ years. The solid curves at each

concentration represent K/U = 1 x $10^4$ while the dashed curves above and below the solid line are K/U = 2 x $10^4$ and K/U = 5 x $10^3$, respectively.

To indicate the possible temperatures and pressures at which melting can be expected within the Moon, the experimentally determined basalt-eclogite melting relations of Yoder and Tilley (1962) out to 30 kilobars and the linear extrapolation to 46 kilobars (lunar central value) are plotted. The diopside melting curve, experimentally obtained by Boyd and England (1963) to 50 kilobars is also included to indicate what is most probably an upper temperature bound for the existence of solid matter. MacDonald (1959) assumed that melting point of diopside indicated the highest temperatures that could be reached in a solid upper mantle. Levin (1962) took melting of the lunar material to be wholly completed when the melting point of dunite is reached. The calculated temperature curves apply until the melting point is reached. At that point the latent heat of fusion should be accounted for.

In Figure 1, melting occurs quite extensively when U = .04 ppm, while no melting occurs in the Moon if U = .01 ppm initially. The critical concentration for melting when $T_o$ = 600°C lies between these limits. The change of K/U ratios from 5 x $10^3$ to 2 x $10^4$ has only a minor effect as is shown for U = .04 ppm.

The results of the calculations are combined in Figure 2 in such a way that the result of an initial uranium concentration and initial temperature distribution can be immediately found. The figure shows the central melting relations at t = 4.5 x $10^9$ years. The final temperature reached at the center of the Moon is plotted against the initial central temperature for various radioactive contents. For example, taking $T_o$ = 600°C and U = .02 ppm,

yields a central temperature of 1550°C after 4.5. The uranium concentrations form a natural third scale which may be used to find the initial temperatures required for final melting.

With the compositional ranges chosen in this study, melting for a lunar model initially at 0°C throughout requires U = 0.03 ppm. For both the adjusted chemical compositions and the chondritic compositions, the melting point of diopside is greatly exceeded indicating extensive melting. If the mean radioactivity of the Moon is depleted compared to the Earth as Ringwood (1966) and others have suggested, then the Moon should not have melted. These compositional changes make possible the explanation of the lunar non-equilibrium shape in terms of a non-extensively melted Moon.

ACKNOWLEDGEMENTS

I am indebted to Dr. Paul W. Gast of Lamont Geological Observatory and Columbia University for suggesting this extension of the lunar thermal history problem and for his helpful discussions. I am also grateful to Dr. John Nafe for critically reading the manuscript. Mr. Chao-Wen Chin of the Goddard Institute for Space Studies assisted with valuable programming assistance.

Figure 1. Temperature versus depth in the moon at $t = 4.5 \times 10^9$ years

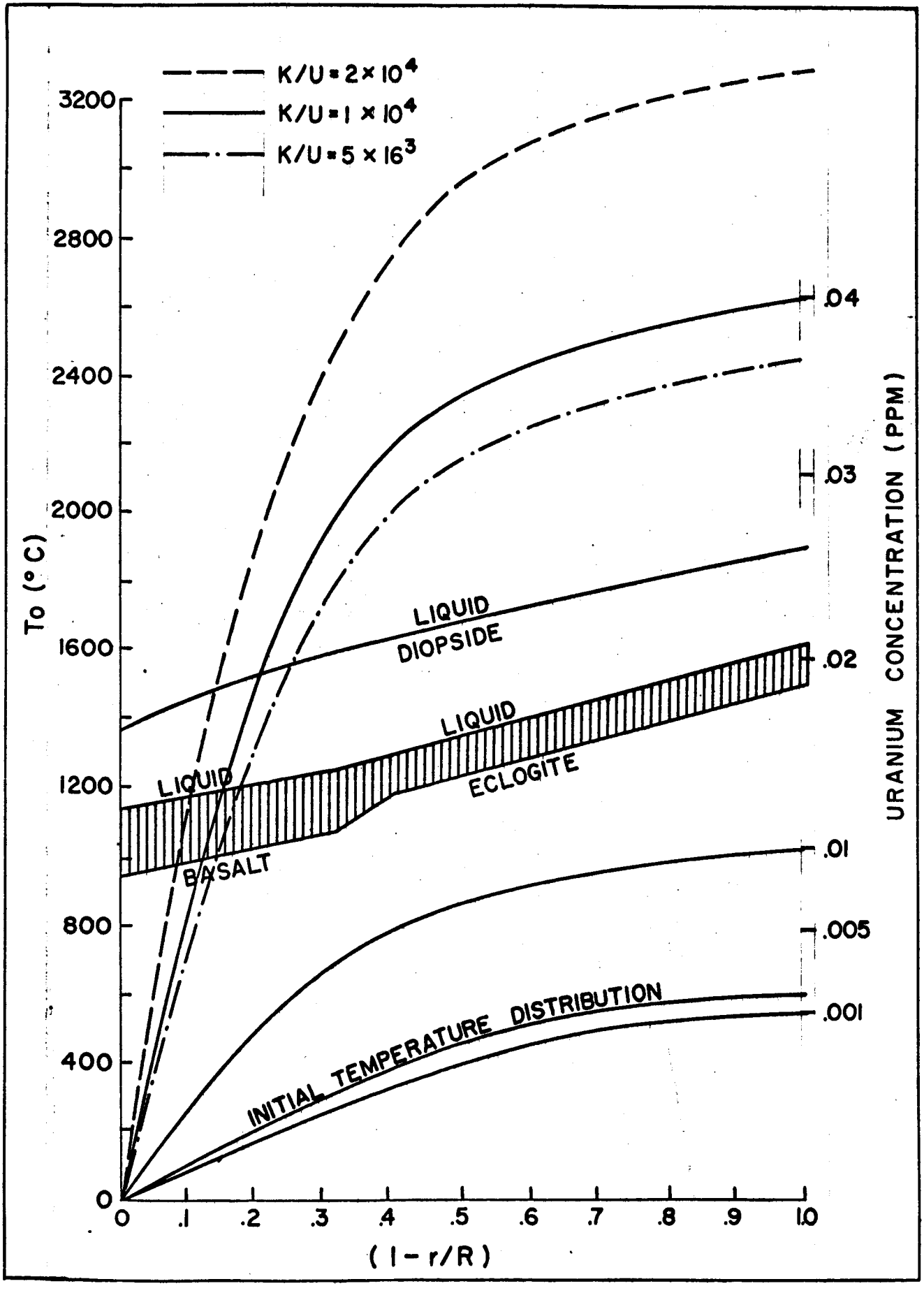
K/U = 2 × 10^4
K/U = 1 × 10^4
K/U = 5 × 16^3
3200
2800
2400
2000
1600
1200
800
400
0
To (°C)
LIQUID
DIOPSIDE
LIQUID
ECLOGITE
LIQUID
BASALT
INITIAL TEMPERATURE DISTRIBUTION
.04
.03
.02
.01
.005
.001
URANIUM CONCENTRATION (PPM)
0
.1
.2
.3
.4
.5
.6
.7
.8
.9
1.0
(1 − r/R)

*FIGURE 1.*

Figure 2. Melting relationships at the center of the Moon at $t = 4.5 \times 10^9$ years. The vertical boundary at approximately 1550°C represents initial melting (the melting of basalt-eclogite) while the boundary at approximately 1850°C represents complete melting (the melting of diopside).

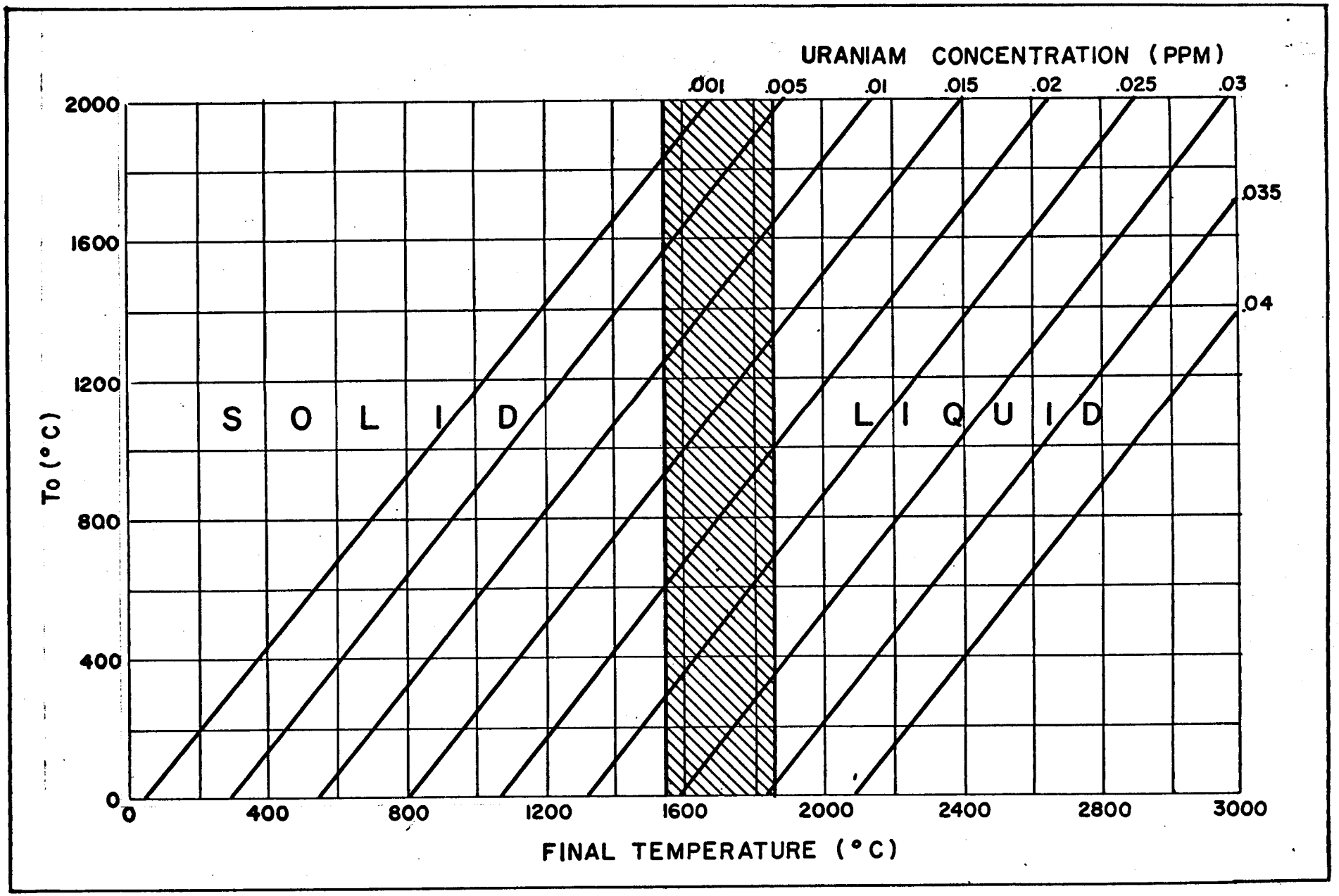
URANIAM CONCENTRATION (PPM)
.001
.005
.01
.015
.02
.025
.03
.035
.04
2000
1600
1200
800
400
0
To (°C)
SOLID
LIQUID
0
400
800
1200
1600
2000
2400
2800
3000
FINAL TEMPERATURE (°C)

*FIGURE 2.*

## REFERENCES


Boyd, F.R., and J. England, The effect of pressure on the melting of diopside, $CaMgSi_2O_6$, and albite, $NaAlSi_3O_8$, in the range up to 50 kilobars, J. Geophys. Res., 68, 311-324, 1963.

Carslaw, H. S. and J. C. Jaeger, Conduction of Heat in Solids, 2nd ed., Oxford University Press, London, 1959.

Gast, P. W., Limitations on the composition of the upper mantle, J. Geophys. Res., 65, 1287-1297, 1960.

Jacobs, J. A., The Earth's interior, in Handbuch der Physik, edited by S. Flugge, Springer-Verlag, Berlin, 1956.

Levin, B. J., The thermal history of the Moon, in The Moon, edited by Z. Kopal and F. K. Mikhailov, Academic Press, London and New York, 1962.

Lubimova, H. A., The thermal history of the earth with consideration of the variable thermal conductivity of the mantle, Geophys. J. Roy. Astron. Soc., 1, 115-134, 1958.

MacDonald, G.J.F., Calculations on the thermal history of the earth, J. Geophys. Res., 64, 1967-2000, 1959.

MacDonald, G.J.F., The dependence of the surface heat flow on the radioactivity of the earth, J. Geophys. Res., 69, 2933-2946, 1964.

Phinney, R. A. and D. L. Anderson, Internal temperatures of the Moon, in Report of Tycho Meeting, Appendix I, prepared by University of Minnesota for NASA, 1965.

Ringwood, A. E., The chemical evolution of the terrestrial planets, Geochim. et Cosmochim. Acta, 30, 41-104, 1966.

REFERENCES (continued)

Tilton, G. R. and G. W. Reed, Radioactive heat production in eclogite and some ultramafic rocks, in Earth Science and Meteorites, compiled by J. Geiss and E. D. Goldberg, 31-44, North Holland Publishing Company, Amsterdam, 1963.

Urey, H. C., The Planets, Yale University Press, 1952.

Urey, H. C., The origin and history of the Moon, in Physics and Astronomy of the Moon, edited by Z. Kopal, pp. 481-523, Academic Press, New York, 1962.

Urey, H. C., A review of atomic abundances on chondrites and the origin of meteorites, Revs. Geophys., 2, 1-34, 1964.

Wasserburg, G. J., G. J. F. MacDonald, F. Hoyle, and W. A. Fowler, The relative contributions of uranium, thorium and potassium to heat production in the earth, Science, 143, 465-467, 1964.

Yoder, H. S. and C. E. Tilley, The origin of basalt magmas: An experimental study of natural and synthetic rock systems, J. Petrol., 3, 342-532, 1962.

# THE PETROLOGY AND GEOCHEMISTRY OF MESOSIDERITES: A PROGRESS REPORT

January 23, 1967

Benjamin N. Powell

# INTRODUCTION

This investigation is concerned with the petrology and geochemistry of the mesosiderite meteorites. Methods of investigation include the following: 1) microscopic examination of polished thin sections and surfaces in transmitted and reflected light; 2) electron probe microanalysis of the same sections; 3) chemical analysis for bulk chemistry and trace elements; 4) oxygen isotope analysis. To date methods (1) and (2) have been applied. Although further investigation involving these two techniques will be pursued, and in this sense this phase of the project is not yet completed, the information obtained thus far in the study will be summarized in this progress report.

At this time single polished thin sections have been obtained of the following mesosiderites: Hainholz, Veramin*, Vaca Muerta, Bondoc, Patwar*, Udei Station*, Lowicz*, Morristown, Estherville*, and Crab Orchard. (Those marked with an asterisk are falls.) It can be seen that 5 of the 7 mesosiderite falls are represented in this list. In this study the compositions of the major silicate phases have been quantitatively determined by electron probe analysis for all of the listed meteorites except Estherville and Crab Orchard. These results are described individually below along with the petrography of the samples.

# ACKNOWLEDGEMENTS

This project has been made possible through the kind cooperation of Mr. V. Manson of the American Museum who provided the materials, of the Institute for Meteorite Research (Smithsonian Institute), where the polished

thin sections were prepared, and of Dr. P. Weiblen of the University of Minnesota, who provided invaluable guidance during the electron probe analysis.

## RESULTS

### Hainholz (find)

The examined portion of Hainholz is characterized by a cataclastic structure, consisting of subhedral to anhedral rectangular to equidimensional grains of orthopyroxene and minor pigeonite and plagioclase suspended in a fine-grained comminuted matrix of the same materials. Opaques (mainly metallic Ni-Fe and troilite) are distributed in disconnected, irregular patches throughout the section. These patches are of varied size and shape, but typically are on the order of 0.5mm in diameter. The larger silicate grains measure from about 0.15mm to 1.5 X 2.5mm. The grains in the groundmass are generally fragmented and angular in appearance and are on the order of 0.04mm.

Exsolution of clinopyroxene is absent in the larger although present in the smaller orthopyroxene grains. The larger pigeonite grains display irregular rims of orthopyroxene, suggesting partial inversion. Rounded inclusions of Ni-Fe, troilite, and chromite have been observed in the larger pyroxene grains.

Margins of the larger pyroxene and plagioclase grains are generally irregular on a fine scale, showing small embayments. Nowhere are these grains seen in direct contact with the opaque areas: there always appears to be some amount of the fine-grained matrix between the two. The larger silicate grains generally display irregular fractures with no apparent separation. These fractures are usually stained yellow to orange-brown, presumably indicating some redistribution of iron in the form of oxides or hydroxides.

Troilite and Ni-Fe in the opaque patches occur in intimate association in irregular grains of varying size and shape. Troilite typically may be in grains on the order of 0.3mm. Chromite is generally euhedral or subhedral, on the order of 0.05mm.

Microprobe analysis gives the following silicate compositions: Orthopyroxene ($En_{70}Fs_{30}$ to $En_{80}Fs_{20}$, not zoned); pigeonite ($En_{60}Fs_{37}Wo_3$); plagioclase (large: $An_{91}$ to $An_{97}$, not zoned; groundmass: $An_{79}$ to $An_{82}$, not zoned). Apatite and tridymite were located in the groundmass by electron probe cathodoluminescence. Olivine is not present in this section.

Veramin* (fall)

The examined section of Veramin is similar to Hainholz in cataclastic structure. Anhedral and fractured grains of orthopyroxene, olivine, and plagioclase are suspended in a finer-grained matrix of the same materials. The size difference between the larger, suspended grains and the matrix grains is not as great as in Hainholz, but is distinct. Ni-Fe occurs in irregular patches some of which are locally connected to give a network on a local scale. However, the opaque distribution is still generally in isolated patches of the order of 1.5 to 2mm. One patch of Ni-Fe measures about 6mm in diameter and contains 1mm "islands" of silicates. The larger silicates are fractured in a manner similar to those in Hainholz.

Toilite, if present at all, is in very small quantities, the opaque material consisting primarily of metallic Ni-Fe. Apatite and tridymite were identified in the non-metallic matrix by probe techniques. Pigeonite appears to be absent.

Probe analyses of the silicates indicate the following compositions: Orthopyroxene (range $En_{69}Fs_{31}$ to $En_{60}Fs_{20}$; generally $En_{75}Fs_{25}$ and not zoned; one grain is zoned, giving $En_{69}Fs_{31}$ in the core, $En_{74}Fs_{26}$ in the rim); plagioclase ($An_{84}$ to $An_{94}$ range, typically $An_{89}$, unzoned). The olivine is Mg-rich and needs to be redetermined.

Vaca Muerta (find)

The examined section of Vaca Muerta possesses a cataclastic structure strongly similar to Veramin. The distribution of opaques is still in irregular patches, although approaching a continuous network. One large patch of Ni-Fe measures about 6 by 12mm and displays Widmanstatten structure. This is visible in the unetched polished surface (see plate 1, the color photomicrograph). The kamacite lamellae are about 0.05mm wide, and the taenite lamellae measure about 0.01mm or less, somewhat finer than the finer octahedrites. Plate 2, a Ni Kα x-ray oscilloscope image of the lamellae, clearly shows the Ni distribution between the two phases. Plate 3 is a Ni Kα x-ray oscilloscope image of a taenite bleb in the same general area of Vaca Muerta. The bleb is about 0.025mm wide. Figure 1 shows the variation in the composition of the taenite by means of a probe traverse analysis. The pattern closely resembles that commonly observed in Widmanstatten lamellae in irons and chondrites.

The margins of the silicate grains are typically embayed and/or corroded where they are in contact with metal. Many grains show a high degree of rounding suggestive of incipient melting.

Troilite and Ni-Fe occur in patches as described, but not as inclusions of one in the other. Troilite occurs within a silicate "island" in the large patch of Ni-Fe.

Probe analyses give the following silicate compositions: orthopyroxene: (range $En_{60}Fs_{40}$ to $En_{72}Fs_{28}$, typically ca. $En_{66}Fs_{34}$, unzoned); plagioclase (range $An_{72}$ to $An_{87}$, typically $An_{80}$); olivine composition is Mg-rich, has yet to be determined quantitatively. Apatite and tridymite were identified by probe techniques. Pigeonite is absent, as is Ca-rich clinopyroxene (except as very minor exsolution from orthopyroxene).

Bondoc (find)

This sample of Bondoc is very highly fractured but shows little or no rotation or transportation of fragments. The material appears shattered but not redistributed. Silicates include primarily orthopyroxene ($En_{68}Fs_{32}$ to $En_{79}Fs_{21}$, unzoned) and plagioclase ($An_{68}$ to $An_{99}$). Olivine and pigeonite are absent in this section. Metallic Ni-Fe is present in minor amounts. The dominant opaque material appears to be iron oxides and/or hydroxides. It is suspected that this sample has been severely affected by terrestrial weathering, although the hand specimen does not clearly suggest this. Additional material is being sought for investigation.

Patwar* (fall)

This section of Patwar shows a strong cataclastic structure with marked differences from the meteorites described above. The gross texture is characterized by multicrystalline fragments and angular single crystal fragments of varied size and shape suspended in a nearly continuous network of Ni-Fe and troilite. The multicrystalline fragments, ranging in size from 2 to 6mm in diameter, consist of twinned pigeonite, plagioclase, tridymite, and minor apatite. Isolated grains of these minerals and of olivine and orthopyroxene range in size from less than 0.2mm up to 2 X 6mm (olivine). In

addition to this material much very fine grained cloudy or dusky material carrying angular silicate grains occurs in isolated patches and bordering the larger multicrystalline fragments. Margins of multicrystalline fragments, of dusky material, and of single crystal fragments are highly embayed and/or corroded where in contact with metal. Many of the smaller isolated grains are rounded as if from melting.

Silicate compositions are varied, although zoning is lacking. Compositions are relatively constant within the multicrystalline fragments but vary slightly from fragment to fragment. Orthopyroxene compositions differ distinctly fro pigeonite compositions with respect to MgO/FeO ratios. (Orthopyroxene does not occur within the multicrystalline fragments.) Some compositions are as follows: pigeonite ($En_{52}Fs_{46}Wo_2$ to $En_{59}Fs_{39}Wo_2$); orthopyroxene ($En_{67}Fs_{33}$ to $En_{76}Fs_{24}$); olivine ($Fo_{64}Fa_{36}$); plagioclase ($An_{89}$ to $An_{93}$).

Troilite and metallic Ni-Fe are in irregular connected patches making a continuous network. Ni-Fe forms one crudely circular patch about 6mm in diameter. Some sort of irregular intergrowth appears to have occurred between troilite and metallic Ni-Fe in places where grains of the two materials are adjacent to one another.

Udei Station * (fall)

The texture in this section is characterized by rounded multicrystalline areas of anhedral equidimensional silicates displaying an aplitic-like texture and single isolated silicate grains suspended in a continuous matrix of Ni-Fe and troilite. Small grains of Ni-Fe, troilite and chromite are present in the multicrystalline areas. Silicates include orthopyroxene (possible pure enstatite), olivine (very Mg-rich) and plagioclase ($An_{16}$ to $An_{18}$). The compositions of the silicates are unusual compared to the other mesosiderites studied (especially the plagioclase) and warrant further investigation.

The margins of the silicate grains are rounded and embayed where in contact with metal. The overall appearance of Udei Station is highly suggestive of a process of liquid metal invasion and disaggregation of solid silicate material with some degree of melting of the latter. Angular, brecciated, cataclastic features are not present in this section of Udei Station as they are in the other meteorites described above. (However, minor yellow-stained fractures are observed in the silicates.)

Lowicz* (fall)

The examined section of Lowicz displays a porphyritic, xenomorphic granular texture. (These terms are used here to describe the physical appearance of the texture without necessarily presuming a truly igneous origin at the moment.) Several large (ca. 6 X 6mm) orthopyroxene grains are contained in a finer-grained matrix of anhedral orthopyroxene and plagioclase with accessory tridymite and apatite. Metallic Ni-Fe occurs in isolated irregular patches typically 3 X 4mm. Finely granular troilite occurs with the Ni-Fe. Exsolution blebs and lamellae of Ca-rich clinopyroxene, sometimes oriented in two directions, are present throughout the smaller orthopyroxene grains and in the rims of the larger ones. The larger orthopyroxenes contain many smaller euhedral to subhedral inclusions of plagioclase in their rims in an ophitic texture. These large orthopyroxenes are compositionally zoned, being enriched in iron in their rims. A typical composition is $En_{83}Fs_{17}$ in the core, $En_{70}Fs_{30}$ in the rim. The plagioclase ranged in composition from $An_{86}$ to $An_{94}$, is most typically $An_{90}$- $An_{94}$, unzoned. Olivine is not present in this section. The larger silicate grains are fractured irregularly, and the fractures are outlined with yellow-brown material. Marked cataclism and brecciation is not observed, however.

Morristown (find)

This sample of Morristown very closely resembles Lowicz as described above with respect to general texture. The large orthopyroxene grains are 1.5 X 3.5mm and have subhedral plagioclase inclusions in thei rims. Clinopyroxene exsolution occurs as in Lowicz. Anhedral plagioclase and orthopyroxene make up the groundmass with accessory apatite and tridymite. Olivine is present in sizeable isolated anhedral grains (up to 1 X 5.4mm) with rounded corners and in a group of anhedral grains on the order of 1mm in diameter. The olivines in the group are twinned. The largest olivine grain (1 X 5.4mm) is untwinned but is zoned from one end to the other ($Fo_{83}Fa_{17}$ to $Fo_{77}Fa_{23}$). The isolated olivine grains and the outer margin of the group are surrounded by a narrow zone of tiny (0.004 X 0.02mm) acicular crystals arranged perpendicular to the grain boundary. (See Plate 4, color photomicrograph.) These have not been identified as yet but are strongly suggestive of a reaction rim.

Metallic Ni-Fe occurs in irregular isolated patches which have some elongation crudely oriented in one direction, parallel to the elongation of the large olivine grain. The silicates are fractured and stained as in Lowicz, but again cataclastic textures are not evident. The orthopyroxenes display slight zoning in the larger grains, typically being $En_{68}Fs_{32}$ in the $En_{63}Fs_{37}$ in the rims. Plagioclase compositions range from $An_{87}$ to $An_{96}$, typically are around $An_{90}$.

## SUMMARY

The above descriptions, although not in complete detail, indicate significant similarities and differences among the mesosiderites studied so far. Cataclism and brecciation of silicates typifies Hainholz, Veramin, Vaca

Muerta, Patwar, and Bondoc. In the first three brecciation and reaction of silicates (resembling basaltic achondrites in mineralogy) with metal with rotation of the former involving no significant transportation is suggested. In Patwar the varied compositions of the silicate "xenoliths" and "xenocrysts" suggests that in addition to brecciation and reaction significant transportation of silicate materials has occurred, either before or after introduction of metal. Bondoc shows evidence of strong cataclism without transportation or even rotation of fragments. Udei Station suggests liquid metal invasion and disaggregation of solid silicate material (resembling certain chondrites in silicate compositions) without any brecciation. Lowicz and Morristown superficially suggest crystallization from a melt or gross recrystallization, with cataclastic textures absent or masked by later events.

More interpretations will be made and the above will doubtless be modified as this investigation proceeds. No doubt many more minor phases will be identified and their meaning, if any, interpreted. The apparent widespread occurrence of tridymite (in all but Bondoc and Udei Station) and the Widmanstatten structure in Vaca Muerta may be significant. Presence or absence of olivine may be of interest, although this may merely reflect the typical inhomogeneity of mesosiderites, something to be determined with further sampling. Chemical analyses and isotope data will doubtless greatly contribute to the interpretation of this information and to the understanding of mesosiderites as a whole.

Plate 1. Widmanstatten structure in Vaca Muerta. The kamacite bands are ca. 0.05mm wide, the taenite, ca. 0.01mm or less.

Plate 2. Ni Kα x-ray oscilloscope image of the Widmanstatten structure in Vaca Muerta (see Plate 1).

affix
plate 3
here

Plate 3: Ni Kα x-ray oscilloscope image of taenite bleb in Vaca Muerta (see Figure 1).

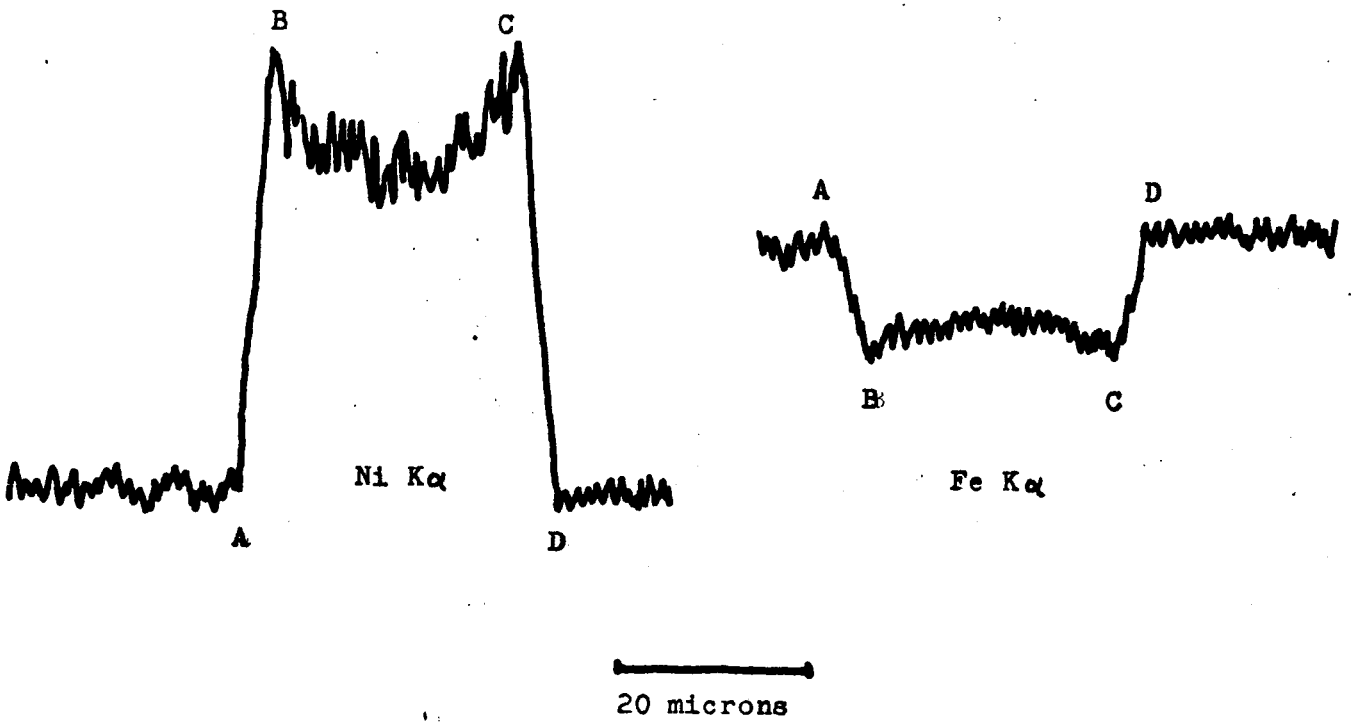


Figure 1: Ni Kα and Fe Kα x-ray relative intensities as a function of distance in a traverse across the taenite bleb illustrated in plate 3.

Plate 4: Acicular crystals in reaction rim around olivine grain in Morristown; the individual needles measure ca. 0.004 by 0.02mm.

Appendix E

For presentation at American Geophysical Union Annual Meeting - 1967

# Disequilibrium of $Ra^{226}$, $Th^{230}$ and $Pb^{210}$ in Historic Volcanic Eruptions

V. B. McConn and P. W. Gast
Lamont Geological Observatory of Columbia University
Palisades, New York

Rock samples from two oceanic islands and from Mt. Vesuvius were analysed for uranium concentration, lead concentration and isotopic composition, $Th^{232}$ and $Th^{230}$ concentration, $Ra^{226}$ activity, and $Pb^{210}$ activity. The islands studied were Tristan da Cunha (five hundred year old Stony Hill flow and 1961 eruption) and Faial, Azores (Capelinhos eruption, 1958).

Both eruptions from Tristan show high lead, uranium and thorium contents. The $Th^{230}/U^{238}$ activity ratio is 1.2 and the $Th^{232}/U^{238}$ weight ratio is between 4.0 and 4.6 indicating enrichment of $Th^{230}$ and possibly $Th^{232}$ at the time of formation of the magma. The Azores samples have concentrations typical of alkali basalts, and have $Th^{230}/U^{238}$ activity ratios of about 1.5 and $Th^{232}/U^{238}$ weight ratios of about 3.6. This indicates that either the source area has an anomalously low Th/U ratio or that the magma forming process was able to separate $Th^{232}$ and $Th^{230}$. The $Ra^{226}/U^{238}$ activity ratios for the different areas average as follows: Tristan, 1.0-1.1; Faial, 2.0; Vesuvius, 8.8. The extremely high $Ra^{226}$ content of Vesuvius is reflected in the $Pb^{210}/U^{238}$ ratio of the rock which is 8.5. The high $Pb^{210}$ content reported for cotunnite from this area (Eberhardt et al., 1955) appears to be due to the radium enrichment in the magma. The $Pb^{210}/U^{238}$ ratio of the Azores samples also reflects their high radium content.

**Appendix F**

For presentation at the American Geophysical Union Annual Meeting - 1967

# Lead and Strontium Isotope Composition of Volcanic Rocks from the South Pacific

I. G. Swainbank and P. W. Gast
Lamont Geological Observatory of Columbia University
Palisades, New York

The lead and strontium isotope composition of volcanic materials from the Society Islands, the Marquesas, Samoa and several of the Austral Islands, have been determined. The seventeen analyses from the Society Islands form a fairly uniform group with respect to both the lead and strontium isotopes. $Pb^{206}/Pb^{204}$ ratios range from 0.7031 to 0.7047. The three samples from the Marquesas are indistinguishable from this group. The rocks from Samoa have lower $Pb^{206}/Pb^{204}$ ratios (18.84) and higher $Sr^{87}/Sr^{86}$ ratios (0.7047). The lead and strontium composition from four samples from Rapa in the Austral Island chain is indistinguishable from the Society Island analyses whilst both the $Pb^{206}/Pb^{204}$ and $Sr^{87}/Sr^{86}$ ratio for a single sample from the Island of Rurutu are high (20.26; 0.7052). The lead composition from two samples from Raratonga in Cook Archipelago fits the primary geochronology.

In addition the $U^{238}/Pb^{204}$ ratios from the Tahiti and Samoa samples have been measured. They are in general high and variable (17.7 to 58.4). No regularity with respect to the $Pb^{206}/Pb^{204}$ ratio has been noted.